Nonadiabatic theory of the superconducting state

M. Botti,[1] E. Cappelluti,[1] C. Grimaldi,[2] and L. Pietronero[1,3]
[1]*Dipartimento di Fisica, Universitàa di Roma "La Sapienza," Piazzale Aldo Moro, 2, 00185 Roma, Italy and INFM, UdR Roma 1, Italy*
[2]*Ecole Polytechnique Fédérale de Lausanne, IPR-LPM, CH-1015 Lausanne, Switzerland*
[3]*CNR, Istituto di Acustica "O. M. Corbino," v. del Fosso del Cavaliere 100, 00133 Roma, Italy*
(Received 25 March 2002; published 22 August 2002)

The nonadiabatic theory of superconductivity has provided a useful tool to investigate the superconducting properties of narrow-band systems where Fermi energy E_F is comparable with the phonon frequencies ω_{ph}. Here we present the extention of nonadiabatic theory to the superconducting state ($T<T_c$) and we derive the generalized Eliashberg equations that include the first nonadiabatic diagrams arising from the breakdown of Migdal's theorem. We show that the opening of the superconducting gap modifies the momentum-frequency structure of the electron-phonon vertex function with respect to normal state. We study the effects of nonadiabatic terms on the superconducting gap Δ and on the ratio $2\Delta/T_c$ in order to relate possible strong-coupling phenomenology, signalized by $2\Delta/T_c>3.53$, and nonadiabatic effects.

DOI: 10.1103/PhysRevB.66.054532 PACS number(s): 74.20.Fg, 63.20.Kr, 74.20.Mn

I. INTRODUCTION

High-T_c superconductors present a complex phenomenology that can be hardly understood within the concept of conventional metals and superconductors. Most remarkable are of course the high values of critical temperatures ranging up to $T_c \simeq 135$ K in cuprates,[1] $T_c \simeq 117$ K in fullerenes doped with field effect,[2] and $T_c \simeq 39$ K in recently discovered MgB_2.[3] While the phononic nature of the pairing seems established in fullerenes and MgB_2, the issue is still debated in the case of the copper oxides.

In principle, such high T_c's could be easily accounted for in the conventional Migdal-Eliashberg (ME) theory by assuming a sufficiently strong superconducting pairing. This simplistic point of view is, however, challenged by a quantitative study. In fact, a crossed analysis of different experimental data, such as the critical temperature T_c, and the isotope coefficient α_{T_c}, and the T_c vs lattice constant a in MgB_2 and in fullerene compounds (where there is a large consensus about the phononic origin of the superconducting pairing), shows that the experimental scenario in these materials would imply extremely large values of the electron-phonon coupling constant λ in the ME framework, respectively, $\lambda \simeq 1.4$–1.7 for MgB_2 (Ref. 4) and $\lambda \simeq 1.3$–2.6 for C_{60} compounds.[5–7] These values of λ appear unrealistic with respect to the stability of these systems towards various structural transitions[8,9] and are, at all cases, in strong disagreement with first-principles calculations that estimate, for instance, $\lambda \simeq 0.7$–0.9 in MgB_2 (Refs. 10–14) and $\lambda \simeq 0.5-0.8$ in C_{60}.[15–19] Normal-state properties present a similar discrepancy between theoretical and experimental estimates of the electron-phonon coupling λ, as the photoemission data in electron doped C_{60} (Refs. 20,21) or the mass enhancement measurements in MgB_2.[22] To summarize this scenario we can say that, from the phenomenological point of view, these high-T_c materials ''look'' like strong-coupling superconductors. However, such strong-coupling phenomenology cannot be simply related to unphysically large values of the *microscopical* λ parameter within a conventional ME framework; it requires a new scenario wherein the realistic value of λ based on local-density approximation (LDA) calculations can account for the strong-coupling phenomenology.

In previous papers we have proposed that nonadiabatic effects can be responsible for the anomalous properties of the high-T_c superconductors.[23–25] Fermi energy is indeed extremely low in all these materials,[26] thus comparable with phonon frequencies. In such a situation the adiabatic assumption, on which Migdal-Eliashberg theory relies, breaks down and new interaction channels arise. This framework is expected to apply in cuprates even if nonphononic mediators are taken into account (spin fluctuations,[27,28] incommensurate charge-density wave,[29] stripes,[30,31] etc) as soon as their energy scales are comparable with the Fermi energy E_F. We have shown that under favorable conditions, which we believe are indeed realized in cuprates, fullerenes, and probably in MgB_2, these types of interactions could enhance the total Cooper pairing and account for the high values of the critical temperature.[4,5,7] The high-T_c superconductivity in fullerenes and MgB_2 results thus being compatible, respectively, with $\lambda \sim 0.4-1$ and $\lambda \sim 0.6-0.9$ are in good agreement with the LDA calculations.

The opening of nonadiabatic channels of interaction can therefore provide a new scenario wherein an effective strong-coupling phenomenology could arise from moderate microscopical λ, at least as regards with the high critical temperature values. We would like to stress again that this apparent strong-coupling phenomenology does not stem from an actual large electron-phonon coupling constant λ, but rather from the effects of the nonadiabatic processes. This distinction has important consequences: (i) the microscopic λ, as said, can be moderate in agreement with first-principles calculations; (ii) there is hence no inconsistency between very high critical temperatures and the absence of any structural instability; (iii) nonadiabatic interactions can affect different physical quantities in different ways: they can, in principle, enhance the total electron-phonon interaction in the particle-particle channel (Cooper pairing) and decrease it in other one-particle (e.g., self-energy) or particle-hole (transport, spin/charge susceptibilities) properties.[32–34]

In this situation it is highly interesting to assess to which extent the nonadiabatic theory of superconductivity can account for the anomalous ''strong-coupling-like'' features of high-T_c materials. Concerning this point it should be reminded that the strong-coupling phenomenology is mainly related to the ratio between superconducting energies (T_c, Δ) and phonon frequencies rather than to the underlying microscopic pairing.[35] One example can be considered, i.e., the gap to critical temperature ratio $R=2\Delta/T_c$. In Migdal-Eliashberg theory, the ratio R increases from the lowest BCS limit of $R=3.53$ to larger values on going from the weak ($\lambda \ll 1$) to the strong ($\lambda \gg 1$) coupling regime. Several detailed studies, however, showed that this trend is essentially related to the superconducting/phonon energy ratio Δ/ω_{ph}:[35]

$$\begin{cases} R \simeq 3.53 & \Delta/\omega_{ph} \ll 1 \\ R > 3.53 & \Delta/\omega_{ph} \sim 1, \end{cases} \tag{1}$$

independent of the microscopic origin of the pairing. The dependence of strong-coupling effects on Δ/ω_{ph} is therefore expected to hold true even in the nonadiabatic framework.

In this paper we provide a generalization of the nonadiabatic theory of superconductivity *into* the superconducting phase to determine the zero-temperature superconducting gap Δ and the ''phenomenological'' strong-coupling parameter Δ/ω_{ph}. We find an interesting competition between two features. On one hand, the opening of nonadiabatic channels increases the ratio Δ/ω_{ph} as well as T_c/ω_{ph} with respect to the adiabatic analysis. On the other hand, the modification of the momentum-frequency structure of the nonadiabatic vertex processes below T_c makes the enhancement of Δ/ω_{ph} less marked than T_c/ω_{ph}. Also, this effect becomes more relevant as the temperature decreases. We anticipate, however, that the first trend is significantly stronger than the second one, and an apparent strong-coupling phenomenology ($\Delta/\omega_{ph} \sim 1$, $2\Delta/T_c > 3.53$) can be consistent with a moderate coupling within the context of the nonadiabatic theory of superconductivity.

The paper is organized as follows. In the following section, we use a perturbative approach to derive a diagrammatic theory of the superconducting state in nonadiabatic regime, and we write the corresponding self-energy equations. In Sec. III, we study the vertex function in the superconducting state and we compare its behavior with that of the same function in the normal state. The last section is devoted to the discussion of some numerical solutions of the self-energy equations.

II. NONADIABATIC PERTURBATION THEORY IN SUPERCONDUCTING STATE

The whole framework of the conventional theory of superconductivity strongly relies on the Migdal's theorem[36] that permits to obtain a closed set of equations for the on-diagonal and off-diagonal parts of the self-energy Σ.[37] In a general way, the self-energy can be expressed as a functional of the electronic Green's function G of the phonon propagator D and of the electron-phonon vertex function Γ: $\Sigma = \Sigma[G,D,\Gamma]$. All the complexity of the problem is therefore contained in the function Γ that includes infinite-order electron-phonon processes, and which is in principle unknown. In his pioneering work, however, Migdal was able to show that for generic exchanged phonon momenta and frequencies ($\mathbf{q}$ and ω) non-zero-order terms of the vertex function were at least proportional to the ratio between phonon and electronic energies ω_{ph}/E_F:[36]

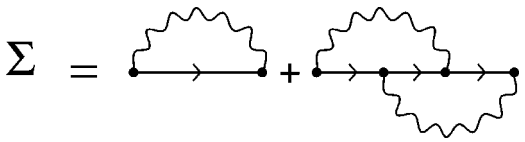

FIG. 1. First-order nonadiabatic expansion of the normal-state self-energy Σ.

$$\Gamma(\mathbf{q},\omega) \simeq g\left[1 + O\left(\lambda \frac{\omega_{ph}}{E_F}\right) + \cdots\right], \tag{2}$$

where ω_{ph} is a measure of the relevant phonon frequencies and E_F is the Fermi energy that defines the characteristic electronic energy scale. In conventional metals and superconductors the adiabatic ratio ω_{ph}/E_F is of order 10^{-3}–10^{-4}, vertex corrections to the lowest order are negligible, and the *total* vertex function can be replaced with its lowest order $\Gamma \simeq g$.

However, fullerenes, cuprates, and MgB_2 do not fulfil the adiabatic requirement, with typical adiabatic ratio about $\omega_{ph}/E_F \sim 0.2-0.8$.[26] In such a situation Migdal's theorem clearly does not apply and higher-order vertex diagrams need unavoidably to be taken into account. Different approaches have been employed in literature to address this issue, based on diagrammatic techniques,[23,24,38,39] Ward's identity[40] or local approximations,[41–43] and generalized also to nonphonon (plasmons,[44] antiferromagnetic fluctuations[45,46]) mediators. In previous papers[23,24] we have pointed out the importance of retaining the whole momentum-frequency structure of the vertex function. In this respect a suitable controlled way to extend the study of electron-phonon interaction in nonadiabatic regime is the use of a perturbation scheme in the parameter $\lambda\omega_{ph}/E_F$, as proposed in Refs. 24 and 25. In those papers a nonadiabatic generalization of the standard ME theory was obtained at $T=T_c$, by expanding the on-diagonal and off-diagonal self-energies to the first order in $\lambda\omega_{ph}/E_F$. In the spirit of such a perturbation theory, only first-order vertex (or cross) corrections were needed to be retained. In a diagrammatic skeleton picture, the normal-state self-energy in nonadiabatic regime would thus appear as shown in Fig. 1.

An important advantage of this approach is the definition of the nonadiabatic theory in terms of skeleton diagrams. This permits to take into account all the orders in the electron-phonon coupling λ without any restriction to the weak-coupling case ($\lambda \ll 1$). Of course, for too strong electron-phonon couplings the use of a perturbation expansion on the parameter $\lambda\omega_{ph}/E_F$ is clearly inadequate, since for λ larger than some model dependent ''critical'' value λ_c nonperturbative polaron trapping becomes dominant.[47–49] Superconductivity in this situation should be better described in terms of (bi)polarons and Bose-Einstein Cooper pair con-

densation should be a better approach. Nevertheless, the present approach is expected to be a good starting point when considering nonadiabatic effects in metals. In that situation the electron-phonon system is expected to acquire characteristic nonadiabatic features, still retaining its metallic behavior. The perturbative approach appears thus to be a useful tool to investigate nonadiabatic effects in this regime and to gain some qualitative insight on this issue. Numerical calculations[43,50] and analytic studies based on Ward's identity[51] show the reliableness of the this approach even beyond the perturbative range of validity provided the polaronic instability is not reached.

The most straightforward way of generalizing a diagrammatic theory in the superconducting state is the use of the Nambu notation, where the electronic Green's functions, self-energies, and vertices are expressed as 2×2 matrices. We assume for the moment that Migdal's theorem holds true even in the Nambu version, namely, *each* matrix component of the vertex corrections is proportional to the adiabatic parameter $\lambda\omega_{\mathrm{ph}}/E_{\mathrm{F}}$ (we shall see later that this is correct). The diagrammatic expression of the Nambu self-energy in the superconducting state, depicted in Fig. 1, is thus identical to that of normal state, where each object (Green's functions, matrix elements) is now replaced by a 2×2 matrix.

Thus the analytic expression of the self-energy reads

$$\begin{aligned}\hat{\Sigma}(\mathbf{k},\omega_n) = {} & T\sum_{\mathbf{p}_1,\omega_m} D(\omega_n-\omega_m)|g_{\mathbf{k}-\mathbf{p}_1}|^2\hat{\tau}_3\hat{G}(\mathbf{p}_1,W_m)\hat{\tau}_3 \\ & + T^2\sum_{\omega_m,\omega_l}\sum_{\mathbf{p}_1,\mathbf{p}_2} D(\omega_n-\omega_m) \\ & \times D(\omega_m-\omega_l)|g_{\mathbf{k}-\mathbf{p}_1}|^2|g_{\mathbf{p}_1-\mathbf{p}_2}|^2 \\ & \times\hat{\tau}_3\hat{G}(\mathbf{p}_1,W_m)\hat{\tau}_3\hat{G}(\mathbf{p}_2,W_l) \\ & \times\hat{\tau}_3\hat{G}(\mathbf{p}_2-\mathbf{p}_1+\mathbf{k},W_{l-m+n})\hat{\tau}_3, \end{aligned} \tag{3}$$

where $\hat{\tau}_i$ are Pauli matrices, $D(\omega_m-\omega_l)$ is the phonon propagator, and W_n are renormalized Matsubara frequencies (which will be defined below).

Nambu notation is particularly efficient in identifying the analytic correspondence of diagrammatic expressions. For practical purpose of calculation it is, however, more convenient to deal separately with on-diagonal and off-diagonal parts of the self-energy, Σ_{11}, Σ_{12}, where the Σ_{ij} represents the (i,j) matrix element of the Nambu self-energy. The diagrammatic expressions of Σ_{11} and Σ_{12} are shown in Fig. 2. After explicitly performing all the matrix products and some careful rearrangement, it is possible to write Eq. (3) as follows:

$$\begin{aligned}\Sigma_{11}(\mathbf{k},\omega_n) = {} & T\sum_{\mathbf{p},\omega_m}\{D(\omega_n-\omega_m)|g_{\mathbf{k}-\mathbf{p}}|^2 \\ & \times[1+P_{\mathrm{nn}}(\mathbf{k},\mathbf{p};W_n,W_m)-2P_{\mathrm{aa}}(\mathbf{k},\mathbf{p};W_n,W_m)] \\ & + C_{\mathrm{aa}}(\mathbf{k},\mathbf{p};W_n,W_m)\}G_{11}(\mathbf{p},W_m), \end{aligned} \tag{4}$$

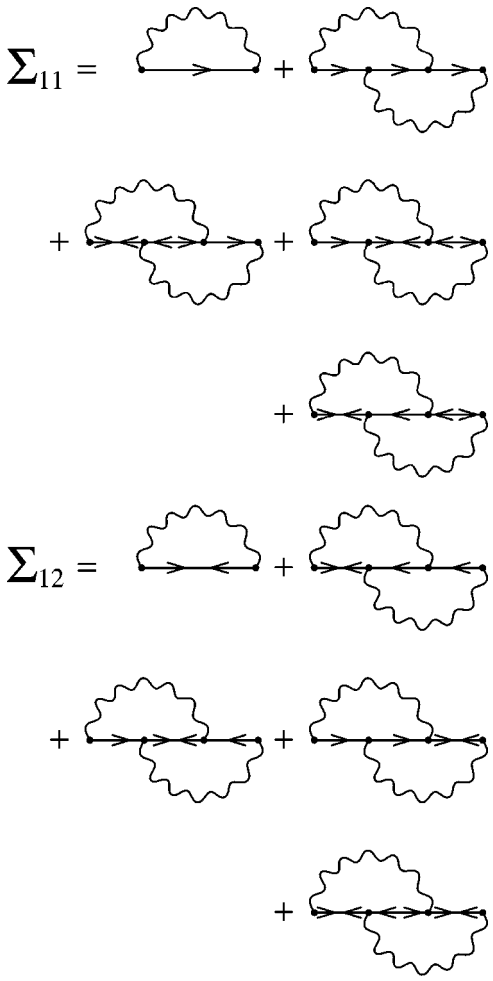

FIG. 2. Diagrammatic expression of the Σ_{11} and Σ_{12} components of the Nambu self-energy in nonadiabatic regime.

$$\begin{aligned}\Sigma_{12}(\mathbf{k},\omega_n) = {} & T\sum_{\mathbf{p},\omega_m}\{D(\omega_n-\omega_m)|g_{\mathbf{k}-\mathbf{p}}|^2 \\ & \times[1+2P_{\mathrm{nn}}(\mathbf{k},\mathbf{p};W_n,W_m)-P_{\mathrm{aa}}(\mathbf{k},\mathbf{p};W_n,W_m)] \\ & + C_{\mathrm{nn}}(\mathbf{k},\mathbf{p};W_n,W_m)\}G_{12}(\mathbf{p},W_m), \end{aligned} \tag{5}$$

where P_{nn}, P_{aa}, C_{nn}, and C_{aa} are, respectively, the electron-phonon vertex and cross contributions arising in nonadiabatic regime. They can be considered as the superconducting state generalization of the vertex and cross functions discussed in Refs. 23–25. Their expressions can be written by introducing the $\tilde{P}_{\mathrm{nn}(aa)}$ and $\tilde{C}_{\mathrm{nn}(aa)}$ functions in the following way:

$$\begin{aligned} & P_{\mathrm{nn}(aa)}(\mathbf{k},\mathbf{k}';W_n,W_m) \\ & \quad = T\sum_l D(\omega_n-\omega_l)\tilde{P}_{\mathrm{nn}(aa)}(\mathbf{k},\mathbf{k}';W_l,W_{l-n+m}), \end{aligned} \tag{6}$$

$$\begin{aligned} C_{\mathrm{nn}(aa)}(\mathbf{k},\mathbf{k}';W_n,W_m) = {} & T\sum_l D(\omega_n-\omega_l)D(\omega_l-\omega_m) \\ & \times\tilde{C}_{\mathrm{nn}(aa)}(\mathbf{k},\mathbf{k}';W_l,W_{l-n-m}). \end{aligned} \tag{7}$$

$\tilde{P}_{\mathrm{nn}(aa)}$ and $\tilde{C}_{\mathrm{nn}(aa)}$ are purely electronic quantities defined as

$$\tilde{P}_{\mathrm{nn}}(\mathbf{k},\mathbf{k}';W_l,W_{l-n+m}) = \sum_{\mathbf{p}} |g_{\mathbf{k}-\mathbf{p}}|^2 G_{11}(\mathbf{p},W_l) G_{11}(\mathbf{p}-\mathbf{k}+\mathbf{k}',W_{l-n+m}), \quad (8)$$

$$\tilde{P}_{\mathrm{aa}}(\mathbf{k},\mathbf{k}';W_l,W_{l-n+m}) = \sum_{\mathbf{p}} |g_{\mathbf{k}-\mathbf{p}}|^2 G_{12}(\mathbf{p},W_l) G_{12}(\mathbf{p}-\mathbf{k}+\mathbf{k}',W_{l-n+m}), \quad (9)$$

$$\tilde{C}_{\mathrm{nn}}(\mathbf{k},\mathbf{k}';W_l,W_{l-n-m}) = \sum_{\mathbf{p}} |g_{\mathbf{k}-\mathbf{p}}|^2 |g_{\mathbf{p}-\mathbf{k}'}|^2 G_{11}(\mathbf{p},W_l) G_{11}(\mathbf{p}-\mathbf{k}-\mathbf{k}',W_{l-n-m}), \quad (10)$$

$$\tilde{C}_{\mathrm{aa}}(\mathbf{k},\mathbf{k}';W_l,W_{l-n-m}) = \sum_{\mathbf{p}} |g_{\mathbf{k}-\mathbf{p}}|^2 |g_{\mathbf{p}-\mathbf{k}'}|^2 G_{12}(\mathbf{p},W_l) G_{12}(\mathbf{p}-\mathbf{k}-\mathbf{k}',W_{l-n-m}). \quad (11)$$

In this definition we made use of the following properties of the G_{ij} propagators: $G_{11}(\mathbf{k},W_n)=G_{22}(-\mathbf{k},-W_n)$, and $G_{12}(\mathbf{k},W_n)=G_{21}(-\mathbf{k},-W_n)$.

Equations (4) and (5) provide the formal generalization of the nonadiabatic theory of superconductivity below T_c. A major role is played by the vertex and cross functions P and C. It is easy to check that for $T\to T_c^-$ vertex and cross contributions related to anomalous the Green's functions, namely, P_{aa} and C_{aa}, vanish, while P_{nn} and C_{nn} reduce to the normal-state vertex and cross functions . We thus simply recover the equations for T_c in nonadiabatic regime (see Refs. 24 and 25), obtained as $T\to T_c^-$ limit of Eqs. (4) and (5).

The nonadiabatic equations of the superconducting state outlined in Eqs. (4) and (5), with the full momentum and frequency dependence, represent a formidable task to be solved from the practical point of view. Useful simplifications arise, however, for an isotropic system, as considered throughout the paper. In that case, the self-energy can be assumed to be weakly momentum dependent and can be thus replaced by its angular-momentum average:

$$\hat{\Sigma}(\mathbf{k},\omega_n) \simeq \langle \hat{\Sigma}(\mathbf{k},\omega_n) \rangle = \hat{\Sigma}(\omega_n). \quad (12)$$

Therefore, the electronic Green's function simply reads

$$\hat{G}(\mathbf{k},W_n) = -\frac{iW_n\hat{I}+\epsilon_{\mathbf{k}}\hat{\tau}_3+\phi_n\hat{\tau}_1}{W_n^2+\epsilon_{\mathbf{k}}^2+\phi_n^2}, \quad (13)$$

where the renormalized Matsubara frequencies W_n are simply related to the bare one as $iW_n = i\omega_n - \Sigma_{11}(\omega_n)$, ϕ_n is the superconducting order parameter, $\phi_n=\Sigma_{12}(W_n)$, and $\epsilon_{\mathbf{k}}$ is the electronic dispersion.

Under the same assumption, the vertex and cross contributions P and C (and correspondingly $\tilde{P}$, $\tilde{C}$) can be shown to depend on fermionic momenta mainly via the only exchanged phonon momentum $|\mathbf{q}|=|\mathbf{k}-\mathbf{k}'|$:[23–25]

$$\tilde{P}_{\mathrm{nn}(aa)}(\mathbf{k},\mathbf{k}';W_l,W_{l-n+m}) \simeq \tilde{P}_{\mathrm{nn}(aa)}(Q;W_l,W_{l-n+m}), \quad (14)$$

$$\tilde{C}_{\mathrm{nn}(aa)}(\mathbf{k},\mathbf{k}';W_l,W_{l-n-m}) \simeq \tilde{C}_{\mathrm{nn}(aa)}(Q;W_l,W_{l-n-m}), \quad (15)$$

where $Q=|\mathbf{q}|/2k_F$. As an immediate consequence, the self-consistent nonadiabatic equations (4) and (5) become a simple convolution.

We can now apply the angular-momentum average, Eq. (12), on each self-energy component. Consider Eqs. (4) and (5). It is straightforward to show that this step corresponds to perform a separate angular average for the nonadiabatic electron-phonon kernel, enclosed in curly brackets, and for the internal Green's function. Thus we end up with the following compact expressions for the nonadiabatic equations of the superconducting state:

$$W_n = \omega_n + 2\lambda T \sum_m \frac{W_m}{\alpha_m} \arctan\left(\frac{E_F}{\alpha_m}\right) \{[1+P_{\mathrm{nn}}(Q_c;W_n,W_m)-2P_{\mathrm{aa}}(Q_c;W_n,W_m)]D(\omega_n-\omega_m)+C_{\mathrm{aa}}(Q_c;W_n,W_m)\}, \quad (16)$$

$$\phi_n = 2\lambda T \sum_m \frac{\phi_m}{\alpha_m} \arctan\left(\frac{E_F}{\alpha_m}\right) \{[1+2P_{\mathrm{nn}}(Q_c;W_n,W_m)-P_{\mathrm{aa}}(Q_c;W_n,W_m)]D(\omega_n-\omega_m)+C_{\mathrm{nn}}(Q_c;W_n,W_m)\}, \quad (17)$$

where we have introduced the renormalized "quasiparticle frequencies" α_n, defined by $\alpha_n=\sqrt{W_n^2+\phi_n^2}$, and the terms $P_{\mathrm{nn}(aa)}(Q_c;W_n,W_m)$, $C_{\mathrm{nn}(aa)}(Q_c;W_n,W_m)$ are the angular averaged vertex and cross functions defined as

$$P_{\mathrm{nn}(aa)}(Q_c;W_n,W_m) = \langle |g_{\mathbf{q}}|^2 P_{\mathrm{nn}(aa)}(\mathbf{q};W_n,W_m) \rangle, \quad (18)$$

$$C_{\mathrm{nn}(aa)}(Q_c;W_n,W_m) = \langle |g_{\mathbf{q}}|^2 C_{\mathrm{nn}(aa)}(\mathbf{q};W_n,W_m) \rangle. \quad (19)$$

The Q_c parameter appearing in Eqs. (18) and (19) gives an estimate of the degree of correlation of the material. While in uncorrelated materials the electron-phonon scattering is indeed known to have only a weak dependence on the phonon

momentum $\mathbf{q}$,[52] strongly correlated systems are characterized by a marked predominance of forward scattering with small momenta $\mathbf{q}$, whereas large momenta are suppressed.[53–55] We modelize this momentum structure as a step function:[23,24]

$$|g_{\mathbf{q}}|^2 \simeq g^2 \left(\frac{2k_F}{q_c}\right)^2 \theta[q_c - |\mathbf{q}|]. \tag{20}$$

The momentum cutoff q_c ($Q_c = q_c/2k_F$) is inversely proportional to the correlation lenght ξ, $q_c \sim 1/\xi$, so that its result is smaller for the more correlated systems and larger for the less correlated ones.

The last ingredient to obtain a closed set of equations of superconductivity in nonadiabatic regime is now the explicit knowledge of the vertex and cross functions $P_{\mathrm{nn}(aa)}(Q_c; W_n, W_m)$ and $C_{\mathrm{nn}(aa)}(Q_c; W_n, W_m)$ in the superconducting state. As we are just going to see, however, we can express these terms in a compact way as functions of the corresponding vertex and cross calculated *in the normal state*.

Let us consider the $\tilde{P}_{\mathrm{nn}}$ function, defined in Eq. (8). It can be easily shown, starting from Eq. (13), that the G_{11} electronic propagator can be written as a linear combination of the two terms: $1/[i\alpha_n - \epsilon_{\mathbf{k}}]$ and $-1/[-i\alpha_n - \epsilon_{\mathbf{k}}]$. Moreover, these two terms have the same form of free-electronic Green's functions, with frequencies $i\alpha_n$ and $-i\alpha_n$ instead of the usual Matsubara frequencies. Indicating with u_n^2 and v_n^2 the coefficients of such linear combination, we can finally write the G_{11} function in the form

$$G_{11}(\mathbf{k}, W_n) = \frac{u_n^2}{i\alpha_n - \epsilon_{\mathbf{k}}} + \frac{v_n^2}{-i\alpha_n - \epsilon_{\mathbf{k}}} = u_n^2 G^0(\mathbf{k}, \alpha_n) + v_n^2 G^0(\mathbf{k}, -\alpha_n). \tag{21}$$

The u_n and v_n quantities can be identified as ''frequency coherence factors'' and are given by

$$u_n = \sqrt{\frac{1 + W_n/\alpha_n}{2}},$$

$$v_n = \sqrt{\frac{1 - W_n/\alpha_n}{2}}. \tag{22}$$

Vertex functions below T_c can now be related in a straightforward way to the vertex function in the normal state by means of the coherence factors u_n, v_n. We obtain, for instance,

$$\tilde{P}_{\mathrm{nn}}(\mathbf{k}, \mathbf{k}'; W_l, W_{l-n+m}) = (u_l^2 u_{l-n+m}^2 + v_l^2 v_{l-n+m}^2)\tilde{P}(\mathbf{k}, \mathbf{k}'; \alpha_l, \alpha_{l-n+m}) + (u_l^2 v_{l-n+m}^2 + v_l^2 u_{l-n+m}^2)\tilde{P}(\mathbf{k}, \mathbf{k}'; \alpha_l, -\alpha_{l-n+m}), \tag{23}$$

where $\tilde{P}(\mathbf{k}, \mathbf{k}'; \alpha_l, \alpha_{l-n+m})$ is the electronic part of the vertex function in the normal state, where the usual Matsubara frequencies must be replaced by the quasiparticle α_n ones. Here we made use of $\tilde{P}(\mathbf{k}, \mathbf{k}'; x, y) = \tilde{P}(\mathbf{k}, \mathbf{k}'; -x, -y)$.

Similar relations apply to $\tilde{P}_{\mathrm{aa}}$. We can express G_{12} as function of the coherence factors as follows:

$$G_{12}(\mathbf{k}, W_n) = -iu_n v_n [G^0(\mathbf{k}, \alpha_n) - G^0(\mathbf{k}, -\alpha_n)], \tag{24}$$

and we obtain

$$\tilde{P}_{\mathrm{aa}}(\mathbf{k}, \mathbf{k}'; W_l, W_{l-n+m}) = (-2u_l v_l u_{l-n+m} v_{l-n+m}) \times [\tilde{P}(\mathbf{k}, \mathbf{k}'; \alpha_l, \alpha_{l-n+m}) - \tilde{P}(\mathbf{k}, \mathbf{k}'; \alpha_l, -\alpha_{l-n+m})]. \tag{25}$$

Equations (23) and (25) hold true also for the cross function substituting C ($\tilde{C}$) for P ($\tilde{P}$) and the frequency α_{l-n-m} for α_{l-n+m}.

Explicit calculations for the vertex and cross functions in the normal state have been provided in Refs. 56 and 34, which we refer for their analytic expressions.

As a last result of this section, we are now in the position to check directly the validity of Migdal's theorem in the superconducting state. In particular, we are going to show that all the first-order nonadiabatic diagrams *in the superconducting state* are at least linear in the adiabatic parameter ω_{ph}/E_F.

We consider the P_{nn} function as a representative case. A similar derivation applies in a straightforward way also to P_{aa} and to the cross functions C_{nn}, C_{aa}, assuring that the results hold true for all the nonadiabatic corrections appearing in Eqs. (16) and (17).

In order to prove the validity of Migdal's theorem, in the superconducting as well as in the normal state, we need to evaluate the $\omega_{\mathrm{ph}}/E_F \to 0$ limit of the vertex function P_{nn} for generic finite values of the exchanged momentum $\mathbf{q}$ ($Q = |\mathbf{q}|/2k_F$) and frequency $\omega = \omega_n - \omega_m$. For simplicity we assume all through the paper that the phonon spectrum is given by a single Einstein mode with frequency ω_0. The task is hugely simplified by using Eqs. (23) and (25) that relate, through the coherence factors, the vertex function P_{nn} (or P_{aa}, C_{nn}, C_{aa}) with the $\tilde{P}$ function in the normal state. Reminding that the coherence factors u_n and v_n do not depend on the phonon properties, the validity of Migdal's theorem in the superconducting state is trivially proven since it reduces to the corresponding one in the normal state.

By using the explicit expression of the vertex function $\tilde{P}(Q, Q_c; W_m, W_n)$ in the normal state for generic exchanged momenta Q and $W_n - W_m$ (Refs. 56 and 34), we obtain

$$\lim_{\omega_0/E_F \to 0} \tilde{P}(Q, Q_c; W_m, W_n) = \lambda \frac{\omega_0}{E_F} \{\pi[\mathrm{sgn}(W_m) - \mathrm{sgn}(W_n)] - 2\}, \tag{26}$$

and, replacing W_n with α_n in Eq. (23),

$$\lim_{\omega_0/E_F\to 0} P_{nn}(Q,Q_c;W_m,W_n)=\lambda\, T\sum_l D(\omega_n-\omega_l)$$
$$\times\frac{\omega_0}{E_F}[-2\pi(u_l^2v_{l-n+m}^2+v_l^2u_{l-n+m}^2)$$
$$-2(u_l^2u_{l-n+m}^2+v_l^2v_{l-n+m}^2+u_l^2v_{l-n+m}^2+v_l^2u_{l-n+m}^2)]. \quad (27)$$

Reminding the definition (22) of the coherence factors, we can write this expression in a more compact form as follows:

$$\lim_{\omega_0/E_F\to 0} P_{nn}(Q,Q_c;W_m,W_n)$$
$$=\lambda\frac{\omega_0}{E_F}T\sum_l D(\omega_n-\omega_l)\left[\pi\left(\frac{W_lW_{l-n+m}}{\alpha_l\alpha_{l-n+m}}-1\right)-2\right], \quad (28)$$

which clearly shows the linear dependence on the adiabatic parameter $\lambda\omega_0/E_F$ of the vertex function also in the superconducting state.

III. STUDY OF THE VERTEX FUNCTION BELOW T_c

In the last section we have derived a closed set of self-consistent equations, Eqs. (16) and (17), which will be numerically solved in the following section to obtain the superconducting properties in the nonadiabatic regime. Before coming to this point, however, we think useful to analyze more closely the momentum-frequency structure of the vertex function in the superconducting state to gain physical insight about the effects of the nonadiabatic corrections. In particular, an important feature to assess is the overall sign of the vertex function, where positive sign is expected to enhance the superconducting pairing and negative sign to suppress it.[23–25]

Vertex function in the normal state was shown to depend in a nontrivial way on the momentum and frequency of the exchanged phonon. The complex structure can be schematized by the static and dynamic limits defined as[23]

$$P^s\equiv\lim_{Q\to 0}\lim_{\omega\to 0}P(Q,Q_c;\omega_m,\omega_n),$$
$$P^d\equiv\lim_{\omega\to 0}\lim_{Q\to 0}P(Q,Q_c;\omega_m,\omega_n). \quad (29)$$

In the normal state the difference of P^s and P^d can be shown to be finite, evidencing a point of nonanalyticity in $(Q=0,\ \omega=0)$. As a representative case the two limits were calculated in Ref. 23 at the lowest order in λ and zero temperature:

$$P^s=-\lambda\frac{\omega_0}{E_F+\omega_0}, \quad (30)$$

$$P^d=\lambda\frac{E_F}{E_F+\omega_0}, \quad (31)$$

where a flat density of state in a half filled system was assumed. Note that a positive sign implies an enhancement of the effective electron-phonon coupling, while a negative one would reduce it.

From Eqs. (30) and (31), we can see that the effects of the nonadiabatic vertex function is not *a priori* defined, but it depends on the specific region in the Q-ω space probed by the electron-phonon interaction. In particular, we can expect that a dominance of forward (small-Q) scattering in the electron-phonon interaction would mainly select the positive part of the vertex terms, leading to a net enhancement of the pairing and an increase of T_c.[24,25] This situation is indeed encountered in strongly correlated systems, such as cuprates and fullerenes, where the electronic correlation suppresses scattering with short-wavelength charge fluctuations.[53–55]

The opening of the superconducting gap for $T<T_c$ changes this scenario in a nontrivial way. On one hand, it removes the point of nonanalyticity at $(Q=0,\ \omega=0)$ by introducing a new energy scale. On the other hand, it also modifies the overall structure of the vertex function. In order to investigate this issue we consider the lowest-order vertex diagrams within a simple BCS model, with no frequency renormalization and with a constant gap:

$$G_{11}(\mathbf{k},\omega_n)=-\frac{i\omega_n+\epsilon_{\mathbf{k}}}{\omega_n^2+\epsilon_{\mathbf{k}}^2+\Delta^2},$$
$$G_{12}(\mathbf{k},\omega_n)=-\frac{\Delta}{\omega_n^2+\epsilon_{\mathbf{k}}^2+\Delta^2}. \quad (32)$$

Let us consider how the opening of the superconducting gap Δ affects the nonadiabatic channels in the Cooper pairing kernel of Eq. (17). We can focalize on the vertex contributions $2P_{nn}-P_{aa}$, which are the leading terms for small Q's. We denote for simplicity $P_\Delta=2P_{nn}-P_{aa}$.

One can show that in this BCS model the vertex function depends on frequencies only via the exchanged phonon frequency $\omega=\omega_n-\omega_m$ explicitly:

$$P_\Delta(Q,\omega)=\frac{\lambda}{2E_FQ}T\sum_l\left[\frac{\omega_0^2}{\omega_l^2+\omega_0^2}\right]\int_{-E_F}^{E_F}d\epsilon\int_{-2E_FQ}^{2E_FQ}dy$$
$$\times\frac{2[\epsilon(\epsilon+y)-\omega_l(\omega+\omega_l)]-\Delta^2}{[\omega_l^2+\epsilon^2+\Delta^2][(\omega_l+\omega)^2+(\epsilon+y)^2+\Delta^2]}, \quad (33)$$

where the electronic dispersion is assumed to be linear, namely: $\epsilon(\mathbf{p}+\mathbf{q})\simeq\epsilon(\mathbf{p})+v_F|\mathbf{q}|\cos\phi=\epsilon(\mathbf{p})+y$, ϕ being the angle between the vectors $\mathbf{p}$ and $\mathbf{q}$ and constant density of states (DOS) was assumed extending from $-E_F$ to E_F.

An interesting feature to be pointed out is that the appearance of the new energy scale driven by Δ removes the nonanalyticity of the vertex function for zero-exchanged momentum frequency, and the static and dynamic limits become equal:

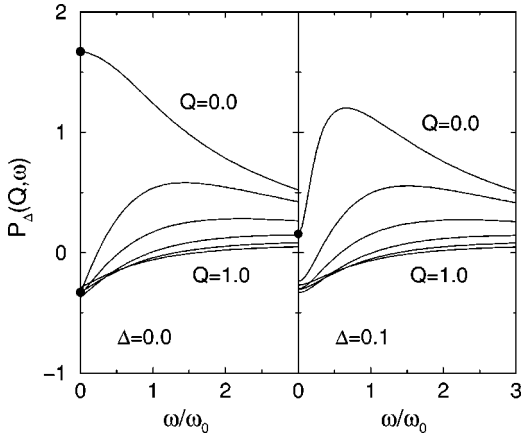

FIG. 3. Frequency structure of the vertex function in the BCS model for different values of the exchanged momentum (from top line to the bottom) $Q=0.0,\ 0.2,\ 0.4,\ldots,1.0$. The adiabatic parameter is here set as $\omega_0/E_F=0.2$, and $\lambda=1$. Left panel refers to the normal state ($\Delta=0.0$) and right panel to the superconducting state ($\Delta=0.1$). Filled circles mark the static and dynamic limits in the normal and superconducting states.

$$P_\Delta^s = P_\Delta^d = \lambda \int_{-E_F}^{E_F} d\epsilon \left[\frac{\omega_0}{2} \frac{2(\omega_0-\epsilon)^2-\Delta^2}{(\omega_0^2-\epsilon^2-\Delta^2)^2} - \frac{\omega_0^2}{\omega_0^2-\epsilon^2-\Delta^2} \frac{3\Delta^2}{4(\epsilon^2+\Delta^2)^{3/2}} - \frac{\omega_0^2}{2(\omega_0^2-\epsilon^2-\Delta^2)^2} \frac{2[\epsilon-\sqrt{\epsilon^2+\Delta^{22}}-\Delta^2]}{\sqrt{\epsilon^2+\Delta^2}} \right]. \tag{34}$$

In Fig. 3 we show the structure of the vertex function involved in the Cooper pairing $P_\Delta(Q,\omega)$ as function of the exchanged frequency ω for different momenta Q in the absence and in the presence of the superconducting gap Δ. Once more, the analysis of the static and dynamic limits (marked with filled circles in figure) can be used as a representative case. Quite generally, they are, respectively, positive and negative in the normal state ($\Delta=0$). We see that the opening of the superconducting gap allows them to collapse to a unique intermediate value. This means that in the positive region of small-Q scattering, characterized by the dynamic limit, the enhancement of the Cooper pairing due to the nonadiabatic vertex corrections is effectively reduced in the superconducting state.

In Fig. 4 the value of the static (dynamic) limit in the superconducting state is plotted as function of the gap magnitude Δ. We see how the opening of the gap suppresses the vertex function. The limit $\lim_{\Delta\to 0} P_\Delta(Q=0,\omega=0)$ can be analytically evaluated from Eq. (34) and gives

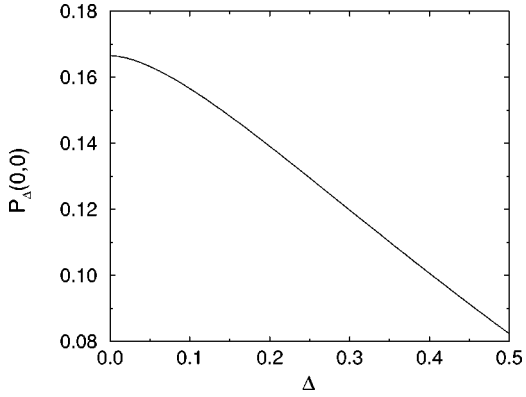

FIG. 4. Dependence of the $P_\Delta(Q=0,\omega=0)$ value of the vertex in the superconducting state as a function of the superconducting gap Δ. Parameter as in previous caption.

$$\lim_{\Delta\to 0} P_\Delta^s = \lim_{\Delta\to 0} P_\Delta^d = \lambda \int_{-E_F}^{E_F} d\epsilon \left[\frac{\omega_0}{(\omega_0+\epsilon)^2} - \frac{3}{2}\delta(\epsilon) + \frac{4\omega_0^2\epsilon}{(\omega_0^2-\epsilon^2)^2} \right] = -\lambda \frac{3\omega_0 - E_F}{2(\omega_0+E_F)}. \tag{35}$$

Note that the positivity of the vertex function at the $(Q=0,\omega=0)$ point is now also affected and the quantity $\lim_{\Delta\to 0} P_\Delta(Q=0,\omega=0)$ becomes, for instance, negative for large enough adiabatic ratios $\omega_0/E_F > 1/3$.

On the ground of the present analysis, we can expect that the superconducting pairing is effectively decreased below the critical temperature with respect to the normal state, which determines, for instance, T_c. This will be indeed confirmed by numerical calculations in the following section.

IV. RESULTS AND DISCUSSION

Equations (16) and (17) represent a set of self-consistent coupled equations, which can be solved numerically by iteration to extract the renormalized frequencies W_n and the superconducting order parameter ϕ_n. Vertex and cross functions $P_{\mathrm{nn}(aa)}$, $C_{\mathrm{nn}(aa)}$ are expressed as a function of W_n and ϕ_n through the coherence factors u_n, and v_n and through the quantity $\tilde{P}(Q_c;W_n,W_m)$ calculated in the normal state.[56,34] The imaginary-axis gap function is thus simply obtained as $\Delta_n=\phi_n/Z_n$ where $Z_n=W_n/\omega_n-1$, and the corresponding "Matsubara" gaps defined as $\Delta_{n=0}$. A simple Einstein phonon with frequency ω_0 and a constant DOS half filled bands were assumed, consistent with the model used in Refs. 24 and 25 for the normal-state nonadiabatic theory calculations. An important parameter we are going to discuss is the ratio $2\Delta/T_c$, where Δ is the physical superconducting gap assumed to be evaluated by experimental techniques. In our theoretical framework the physical gap $\Delta(T)$ can be obtained from Δ_n via the analytical continuation on the real axis, $\lim_{i\omega_n\to\omega+i\delta}\Delta_n \equiv \Delta(\omega,T)$, and through the relation

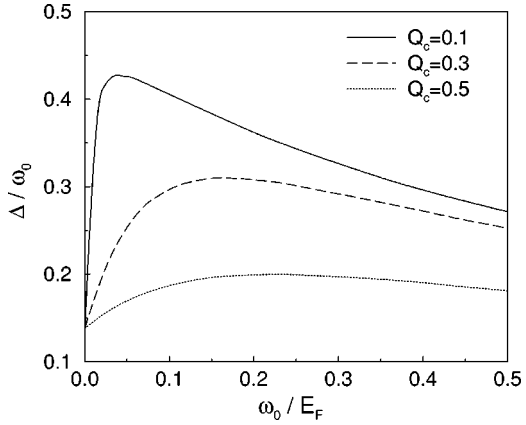

FIG. 5. Superconducting gap in units of ω_0, Δ/ω_0 as function of the adiabatic parameter ω_0/E_F in the nonadiabatic theory for $\lambda=0.7$ and different Q_c's is shown.

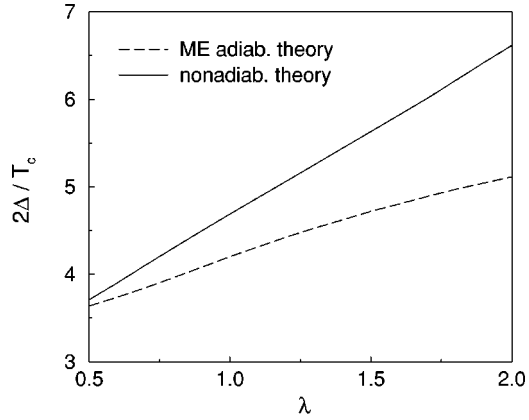

FIG. 6. Ratio $2\Delta/T_c$ as a function of λ for the Migdal-Eliashberg adiabatic theory and the nonadiabatic one ($\omega_0/E_F=0.2$, $Q_c=0.1$).

$$\Delta(T)=\mathrm{Re}\{\Delta(\omega=\Delta(T),T)\}. \tag{36}$$

The zero-temperature physical gap Δ is obtained as $\Delta(T=0)$, whereas the zero-temperature "Matsubara" gap Δ_0 is equivalent to $\Delta_0=\lim_{T\to 0}\Delta_{n=0}=\Delta(\omega=0,T=0)$. Discrepancies between Δ and Δ_0 arise in the strong-coupling regime when the superconducting energy scale Δ is comparable to the frequency structure of $\mathrm{Re}[\Delta(\omega)]$: $\Delta\sim\omega_0$.[35] In this perspective we have performed a numerical comparison between the physical gap Δ and the imaginary-axis gap Δ_0. The discrepancy between Δ and Δ_0 was found to be less than 9% in the region $3.53<2\Delta/T_c<6$, and less than 2% for $2\Delta_0/T_c\simeq 4$. Numerical solutions of the superconducting equations in imaginary axis provide therefore a quite good evaluation of the physical gap Δ. On this basis we shall use Δ_0, calculated from the solution of Eqs. (16) and (17), to evaluate the physical gap and the ratio $2\Delta/T_c$ in the nonadiabatic regime.

The dependence of the superconducting gap as function of the adiabatic ratio ω_0/E_F is shown in Fig. 5. The behavior is quite similar to the corresponding dependence of T_c. In particular, we find that the superconducting gap is significantly enhanced by the nonadiabatic interaction with respect to the Migdal-Eliashberg case ($\omega_0/E_F=0$). The enhancement is more marked for smaller Q_c where the positive region of the vertex function is mainly probed. Note that the increase of Δ/ω_0 with respect to the adiabatic case is alone expected to drive the system in an "effective" strong-coupling regime ($\Delta/\omega_0\sim 1$) that is now, however, not related with a particularly large λ. This is indeed shown in Fig. 6 where the ratio $2\Delta/T_c$ is plotted as function of λ for both the adiabatic and the nonadiabatic theories.

Figure 6 shows that large values of the strong-coupling ratio $2\Delta/T_c$ can be recovered in the nonadiabatic theory by relatively smaller values of λ than needed in the standard ME theory. For instance, $2\Delta/T_c=5$ is compatible with $\lambda=1.2$ whereas it corresponds to $\lambda\simeq 1.8$ in Migdal-Eliashberg framework. From the phenomenological point of view, however, the microscopical electron-phonon coupling λ is not an accessible parameter. A much more useful investigation is the comparison between the ratios $2\Delta/T_c=5$ in the adiabatic and nonadiabatic theories for *fixed critical temperatures* T_c.

According to the analytic study of the preceding section, we expect the superconducting pairing to be decreased by vertex corrections in the superconducting state *with respect to* the normal one. This is confirmed by our numerical calculations. In Fig. 7 we show the temperature evolution of the superconducting gap as obtained by the present nonadiabatic theory including vertex contributions (filled circles) and by the adiabatic Migdal-Eliashberg theory (empty circles). In order to have a direct comparison of the gap values the microscopic parameters of both the adiabatic and nonadiabatic theories were constrained to reproduce the same fixed value of T_c. The required values of λ are shown in the inset for $\omega_0/E_F=0.2$ ($Q_c=0.1$ in the nonadiabatic case). Larger values of λ correspond to higher T_c/ω_0. Figure 7 shows that the nonadiabatic theory predicts $2\Delta(T)/T_c$ curves that are always lower than the ME adiabatic ones.

This result can appear in contradiction with Fig. 6, where nonadiabatic effects were shown to enhance $2\Delta/T_c$. In order

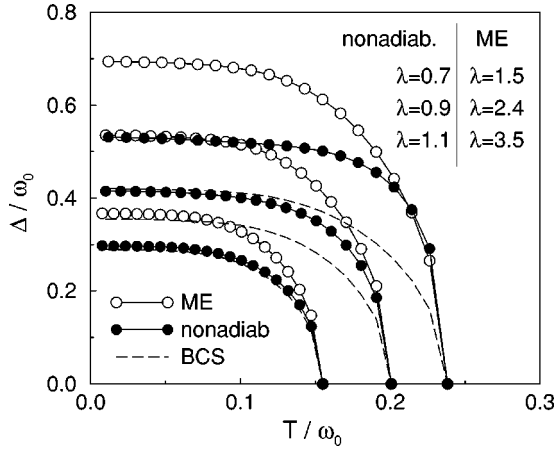

FIG. 7. Temperature evolution of the superconducting gap Δ, in units of ω_0, for the Migdal-Eliashberg adiabatic theory and the nonadiabatic one ($\omega_0/E_F=0.2$, $Q_c=0.1$). Also, dashed lines represent the weak-coupling BCS case.

to understand this apparent discrepancy, it is important to distinguish two different effects. Let us consider a fixed λ. In this case the opening of nonadiabatic channels is known to enhance T_c with respect to the adiabatic theory. This effect drives in general the system towards a strong-coupling limit since the parameter T_c/ω_0, which rules the strong-coupling effects, is correspondingly enhanced. On the basis of this argument, we can expect $2\Delta/T_c$ to be stronger in the nonadiabatic theory than in the Migdal-Eliashberg one, as confirmed by Fig. 6. On the other hand, the detailed analysis of the present paper has shown that the opening of the superconducting gap deeply modifies the vertex function and decreases the strength of the nonadiabatic pairing with respect to the normal state. The ratio $2\Delta/T_c$ is correspondingly reduced.

Thus the two effects act in opposite directions. The total balance between these two effects is better pointed out in Fig. 7. Here the enhancement of the strong-coupling phenomenology driven by the increase of T_c/ω_0 is absent since the microscopic parameters were chosen to reproduce the same value of T_c/ω_0 for both the adiabatic and nonadiabatic theories. We see that $\Delta(T=0)$ is significantly enhanced in the Migdal-Eliashberg case with respect to the weak-coupling BCS limit (dashed lines). This is only due to the finite value of T_c/ω_0, which gives arise to strong-coupling phenomenology ($2\Delta/T_c > 3.53$). This contribution is thus the same in both the theories. The negative role of the opening of the superconducting gap in the nonadiabatic vertex function can be, on the other hand, isolated by comparing $\Delta(T=0)$ in the nonadiabatic theory with the adiabatic result. This comparison shows that the enhancement of $2\Delta/T_c$ due to finite T_c/ω_0 is partially, *but not completely*, suppressed. In particular, we can still observe a significant increase of $\Delta(T=0)$ in the nonadiabatic theory with respect to the BCS result.

We are now in the position to ask us how taking into account the onset of nonadiabatic channels affects the phenomenologic analysis of the experimental data. In particular, we are interested in the basic issue: what can be inferred from the experimental values T_c and $2\Delta/T_c$ about the microscopic coupling λ in the framework of nonadiabatic theory?

In order to answer this simple question we consider a representative example inspired by the cuprates. We would like to stress that this example should be considered just a suitable tool to illustrate how the analysis of experimental data is affected in the nonadiabatic theory, while the microscopic origin of superconductivity in cuprates is still debated. We thus analyzed a half filled system with Fermi energy (half bandwidth) $E_F=0.3$ eV and critical temperature $T_c=100$ K. We considered for simplicity an Einstein phonon spectrum with energy ω_0. The frequency ω_0 was thus determined as a function of the electron-phonon coupling λ to give $T_c=100$ K, and the superconducting gap Δ was then calculated. The results are shown in Fig. 8 where $2\Delta/T_c$ and ω_0 are plotted as a function of λ for different values of Q_c (solid line from the left to the right): 0.1,0.3,0.5. For comparison, the data corresponding to a Migdal-Eliashberg analysis are also shown (dashed line).

For a given value of $2\Delta/T_c$, assumed to be inferred from experimental measurements, let us say $2\Delta/T_c=5$, and given

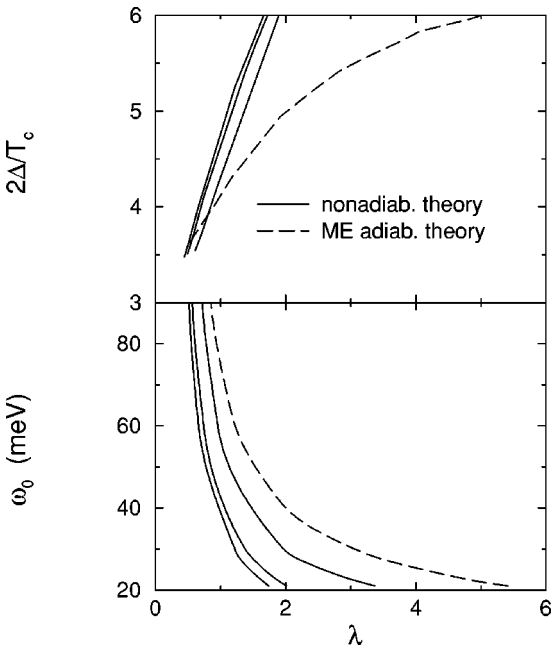

FIG. 8. Ratio $2\Delta/T_c$ (top panel) and phonon frequency ω_0 (bottom panel) constrained to reproduce $T_c=100$ K and $E_F=0.3$ eV. Solid lines are for nonadiabatic theory with (from left to right line) $Q_c=0.1$, 0.3, 0.5. Dashed line represents Migdal-Eliashberg theory.

a value of $T_c=100$ K, we find in the nonadiabatic theory an electron-phonon coupling $\lambda\simeq 1.1$ for $Q_c=0.1$, significantly smaller than $\lambda\simeq 2.0$ estimated within the Migdal-Eliashberg framework. Note that such a discrepancy does not stem from a substantially different phonon energy scale ($\omega_0\simeq 40$ meV in ME theory, $\omega_0\simeq 34$ meV in the nonadiabatic one). We can thus relate the origin of these different results to the onset of nonadiabatic channels in the superconducting pairing. In particular, our results point out that a strong-coupling phenomenology (high T_c, large values of the ratio $2\Delta/T_c$) is *compatible* in a natural way in the nonadiabatic scenario with small values of the electron-phonon coupling λ.

We would like to stress once more that this statement does not imply that nonadiabatic superconductivity *unavoidably* leads to large value of the ratio $2\Delta/T_c$, as it is confirmed by Fig. 8 itself, where the same $T_c=100$ K corresponds to much lower values of $2\Delta/T_c$ (~ 3.53) if the characteristic phonon frequency ω_0 is increased.

V. CONCLUSIONS

In this paper, we have afforded the extension of the nonadiabatic theory of superconductivity within the superconducting state at $T<T_c$. We have shown the validity of a perturbative approach based on a small ω_{ph}/E_F expansion even in the superconducting state. The nonadiabatic equations for $T<T_c$ have been derived by means of a diagrammatic approach. It has been shown that a crucial role is played by the opening of the superconducting gap Δ in the nonadiabatic vertex diagrams. This removes the nonanalytic-

ity at $Q=0$, $\omega=0$ and modifies the overall momentum structure of the vertex function. The generalized equations of the superconducting state are numerically solved to evaluate the superconducting gap Δ in the nonadiabatic scenario. As a physical consequence of our analysis we have shown that a strong-coupling phenomenology is naturally accounted for in the nonadiabatic theory for small values of the electron-phonon coupling λ.

[1] N. M. Plakida, *High Temperature Superconductivity: Experiments and Theory* (Springer-Verlag, Berlin, 1995).
[2] J.H. Schön, Ch. Kloc, and B. Batlogg, Science **293**, 2431 (2001).
[3] J. Nagamatsu, N. Nakagawa, T. Muranaka, Y. Zenitani, and J. Akimitsu, Nature (London) **410**, 63 (2001).
[4] E. Cappelluti, S. Ciuchi, C. Grimaldi, L. Pietronero, and S. Strässler, Phys. Rev. Lett. **88**, 117003 (2002).
[5] E. Cappelluti, C. Grimaldi, L. Pietronero, and S. Strässler, Phys. Rev. Lett. **85**, 4771 (2000).
[6] E. Cappelluti, C. Grimaldi, L. Pietronero, S. Strässler, and G.A. Ummarino, Eur. Phys. J. B **21**, 383 (2001).
[7] P. Paci, E. Cappelluti, C. Grimaldi, L. Pietronero, and S. Strässler, cond-mat/0201334 (unpublished).
[8] P. B. Allen and B. Mitrović in *Solid State Physics*, edited by H. Ehrenreich, F. Seitz, and D. Turnbull (Academic, New York, 1982), Vol. 37.
[9] P. W. Anderson and C. C. Yu, in *Highlights of Condensed Matter Theory*, Proceedings of the International School of Physics ''Enrico Fermi,'' Course LXXXIX, edited by F. Bassani and M. Tosi (North-Holland, New York, 1985).
[10] J. Kortus, I.I. Mazin, K.D. Belashchenko, V.P. Antropov, and L.L. Boyer, Phys. Rev. Lett. **86**, 4656 (2001).
[11] J.M. An and W.E. Pickett, Phys. Rev. Lett. **86**, 4366 (2001).
[12] Y. Kong, O.V. Dolgov, O. Jepsen, and O.K. Andersen, Phys. Rev. B **64**, 020501 (2001).
[13] K.-P. Bohnen, R. Heid, and B. Renker, Phys. Rev. Lett. **86**, 5771 (2001).
[14] H.J. Choi, D. Roundy, H. Sun, M.L. Cohen, and S.G. Louie, Phys. Rev. B **66**, 020513 (2002).
[15] C.M. Varma, J. Zaanen, and K. Raghavachari, Science **254**, 989 (1991).
[16] M. Schluter, M. Lannoo, M. Needeles, G.A. Baraff, and D. Tománek, Phys. Rev. Lett. **68**, 526 (1992).
[17] M. Schluter, M. Lannoo, M. Needels, G.A. Baraff, and D. Tománek, J. Phys. Chem. Solids **53**, 1473 (1992).
[18] J.C.R. Faulhaber, D.Y.K. Ko, and P.R. Briddon, Phys. Rev. B **48**, 661 (1993)
[19] V.P. Antropov, O. Gunnarsson, and A.I. Liechtenstein, Phys. Rev. B **48**, 7651 (1993).
[20] O. Gunnarsson, H. Handschuh, P.S. Bechthold, B. Kessler, G. Ganteför, and W. Eberhardt, Phys. Rev. Lett. **74**, 1875 (1995).
[21] O. Gunnarsson, Rev. Mod. Phys. **69**, 575 (1997).
[22] Ch. Wälti, E. Felder, C. Degen, G. Wigger, R. Monnier, B. Delley, and H. R. Ott, Phys. Rev. B **64**, 172515 (2001).
[23] L. Pietronero, S. Strässler, and C. Grimaldi, Phys. Rev. B **52**, 10 516 (1995).
[24] C. Grimaldi, L. Pietronero, and S. Strässler, Phys. Rev. B **52**, 10 530 (1995).
[25] C. Grimaldi, L. Pietronero, and S. Strässler, Phys. Rev. Lett. **75**, 1158 (1995).
[26] Y.J. Uemura, A. Keren, L.P. Le, G.M. Luke, B.J. Sternlieb, W.D. Wu, J.H. Brewer, R.L. Whetten, S.M. Huang, S. Lin, R.B. Kaner, F. Diederich, S. Donovan, G. Grüner, and K. Holczer, Nature (London) **352**, 605 (1991).
[27] J. Rossat-Mignod, L.P. Regnault, C. Vettier, P. Bourges, P. Burlet, J.Y. Henry, and G. Lapertot, Physica C **185-189**, 86 (1991).
[28] P. Monthoux and D. Pines, Phys. Rev. B **50**, 16015 (1994).
[29] C. Castellani, C. Di Castro, and M. Grilli, Phys. Rev. Lett. **75**, 4650 (1995).
[30] V.J. Emery and S.A. Kivelson, Physica C **235**, 189 (1994).
[31] C. Castellani, C. Di Castro, and M. Grilli, Z. Phys. B: Condens. Matter **103**, 137 (1997).
[32] C. Grimaldi, E. Cappelluti, and L. Pietronero, Europhys. Lett. **42**, 667 (1998).
[33] C. Grimaldi and L. Pietronero, Europhys. Lett. **47**, 681 (1999).
[34] E. Cappelluti, C. Grimaldi, and L. Pietronero, Phys. Rev. B **64**, 125104 (2001).
[35] For a review see, for instance, J.P. Carbotte, Rev. Mod. Phys. **62**, 1027 (1990), and references therein.
[36] A.B. Migdal, Zh. Eksp. Teor. Fiz. **34**, 1438 (1958) [Sov. Phys. JETP **7**, 996 (1958)].
[37] G.M. Eliashberg, Zh. Eksp. Teor. Fiz. **38**, 966 (1960) [Sov. Phys. JETP **11**, 696 (1960)].
[38] V.N. Kostur and B. Mitrović, Phys. Rev. B **48**, 16 388 (1993).
[39] V.N. Kostur and B. Mitrović, Phys. Rev. B **50**, 12 774 (1994).
[40] Y. Takada, Phys. Rev. B **52**, 12 708 (1995).
[41] H.R. Krishnamurthy, D.M. Newns, P.C. Pattnaik, C.C. Tsuei, and C.C. Chi, Phys. Rev. B **49**, 3520 (1994).
[42] J.K. Freericks, E.J. Nicol, A.Y. Liu, and A.A. Quong, Phys. Rev. B **55**, 11 651 (1997).
[43] A. Deppeler and A.J. Millis, Phys. Rev. B **65**, 100301 (2002).
[44] M. Grabowski and L.J. Sham, Phys. Rev. B **29**, 6132 (1984).
[45] A.V. Chubukov, P. Monthoux, and D.K. Morr, Phys. Rev. B **56**, 7789 (1997).
[46] I. Grosu and M. Crisan, Phys. Rev. B **49**, 1269 (1994).
[47] A.S. Alexandrov and P.P. Edwards, Physica C **331**, 97 (2000).
[48] D. Feinberg, S. Ciuchi, and F. de Pasquale, Int. J. Mod. Phys. B **4**, 1317 (1990).
[49] S. Ciuchi, F. de Pasquale, F. Fratini, and D. Feinberg, Phys. Rev. B **56**, 4494 (1997).
[50] M. Capone, S. Ciuchi, and C. Grimaldi, Europhys. Lett. **42**, 667 (1998).
[51] L. De Angelis, E. Cappelluti, C. Grimaldi, and L. Pietronero, (to be published).
[52] G. Grimvall, *The Electron-Phonon Interaction in Metals* (North-Holland, New York, 1981).
[53] M. Grilli and C. Castellani, Phys. Rev. B **50**, 16 880 (1994).
[54] R. Zeyher and M.L. Kulić, Phys. Rev. B **53**, 2850 (1996).
[55] M.L. Kulić, Phys. Rep. **338**, 1 (2000).
[56] M. Scattoni, C. Grimaldi, and L. Pietronero, Europhys. Lett. **47**, 588 (1999).